WORCESTER POLYTECHNIC INSTITUTE

Progress Towards a Higher Throughput Uniaxial Stretch Platform with Tunable Stiffness for Mechanobiology Experiments

by

Leo B. Sutter

A thesis submitted in partial fulfillment for the degree of

Master of Science in Biomedical Engineering

August 2020

Approved:

_____

Kristen Billiar, PhD

_____

Qi Wen, PhD

_____

Adriana Hera, PhD

Outline

Abstract

Calcific aortic valve disease (CAVD) is a disease in which the heart valve leaflets undergo calcification an eventually lose the ability to open and close. Currently the only treatment options for this disease are surgical [1]. Mechanical factors are very important in the progression of CAVD [2-4]. Previous work in our lab has modeled this disease by micropatterning circular aggregates of valvular interstitial cells into circular aggregates on a tunable stiffness substrate [5]. Calcification and apoptosis (which is a cause of calcification) were measured in this model and found to be higher in the center of the aggregates and lower around the edges of the aggregates. Stresses in the aggregate model have been found to be higher on the edge of the aggregates and lower in the centers [5]. We hypothesize that the lower stress state of cells in the center of the aggregates is responsible for the higher calcification and apoptosis. One way to test this is to apply cyclic stretch, which has been shown to raise the stress in the center of the aggregates [6]. The goal of this project is to design an experimental system to apply cyclic stretch to aggregates micropatterned onto a tunable stiffness substrate. Different micropatterning techniques which pattern collagen onto polyacrylamide are attempted and evaluated, along with techniques to bind polyacrylamide to PDMS to enable the application of stretch. Experiments with stretchable micropatterned aggregates are performed in order to validate this system. A technique to polymerize polyacrylamide on a commercially available stretchable multi-well silicone plate is optimized and these gels are characterized for their storage modulus and surface features.

Introduction

Calcific aortic valve disease is a disease which is characterized by calcified nodules in the leaflets of the heart valve, which eventually prevent the heart valve from opening properly and causes regurgitation of blood within the valve. During the progression of the disease, there will be stiffening and thickening of the leaflets. Cartilage and bone are sometimes seen in the calcifying tissue. CAVD is expected to affect 4.5 million people by 2030. Cell death by apoptosis or necrosis, as well as osteogenic differentiation, are thought of as potentially involved in the progress of CAVD [1].

There is strong evidence that CAVD is a mechanically regulated disease [2-4]. For example, mechanical strains have been shown to increase calcification in vitro and ex vivo [2, 3]. The microenvironment in the heart valve, and in particular the stiffness, is likely an important factor in CAVD progression. Stiffness can regulate valvular interstitial cell differentiation into osteoblasts or into myofibroblasts [4].

Stretch and stiffness are important parameter for mechanobiology studies in general, in addition to being important in CAVD. Stretch is known to influence the cytoskeleton in various ways [7, 8]. Stretch can influence the differentiation of cells [9, 10]. It also can affect the alignment of cells. Cells tend to align perpendicular to stretch in 2D culture and parallel to stretch in 3D culture [8, 11]. It is also known that substrate stiffness is also an important parameter for influencing cell behavior [8, 12, 13]. Cell stiffness and the degree to which a cell spreads out on a substrate are known to be affected by substrate stiffness [13]. Differentiation is also affected by substrate stiffness [12]. Cell response to stretch changes for different stiffnesses [8], making it valuable to be able to both control stiffness and apply stretch simultaneously.

It has been shown in vitro that valvular interstitial cells have a tendency to aggregate before undergoing apoptosis and calcification [2]. One way to study the mechanical behavior of cells is through the use of micropatterned aggregates. One thing that makes aggregates (sometimes referred to as cell islands) a useful tool is their nonuniform mechanical environment. It has been found that micropatterned aggregates have higher traction stresses at the edges than in the center, that markers of proliferation and differentiation follow these patterns, and that cyclic stretch can elevate the stress in the center and thereby alter the proliferation and differentiation profiles [6]. Note that stresses in the cyclically stretched aggregates were not measured directly, but were estimated using a finite element model informed by stresses measured in static aggregates [6]. Previous work in our group has involved using aggregates as a model for CAVD. Traction stresses were found to be higher on the edges, consisted with previously mentioned data. It was also found that there was a threshold stiffness above which calcification was higher (but did not further increase with stiffness) and below which it was lower. Apoptosis (which can be a cause of calcification) and calcification were both found to be higher in the center of the aggregates than in the edges [5]. This previous work was with static aggregates, the effect of stretch was not studied. We hypothesize that applying cyclic stretch to the aggregates will raise the stress in the center of the aggregates and decrease apoptosis and calcification in the aggregates.

Therefore, it is desirable to create a system in which stretch can be applied to aggregates in order to test this hypothesis. Since stiffness is an important factor in CAVD [2-4], being able to tune the substrate stiffness in the system would also be beneficial. Polyacrylamide gel is a hydrogel which is used in mechanobiology due to its tunable stiffness and has previously been attached to PDMS in order to facilitate stretching [14-16].

The goal of this project is to develop a system which will enable the application of cyclic stretch to micropatterned aggregates on tunable stiffness substrates. With this system, we will be able to measure the effect of cyclic stretch on disease progression in the model and measure the effect of cyclic stretch on traction stresses in aggregates, which has not been done previously. The development of this protocol consists of three main areas, which are outlined in Figure 1. The first is micropatterning the gel while binding it to a PDMS well. Indirect microcontact printing is the main method used here to do so; however, other micropatterning techniques are also attempted. Next, experiments with aggregates formed in larger PDMS wells are performed in order to demonstrate the analysis techniques that will be used for later experiments. The final part of the project is forming gels on the CellScale silicone plate. The CellScale MCFX is a device which allows for uniaxial testing of a multi-welled silicone plate, which allows for up to 16 different experiments to be conducted simultaneously [17]. This significantly improves throughput over previous single-well studies. This part of the project includes developing a reliable procedure for binding them to it based off previously established methods [14], as well as characterizing the stiffness and roughness of the resulting gels.

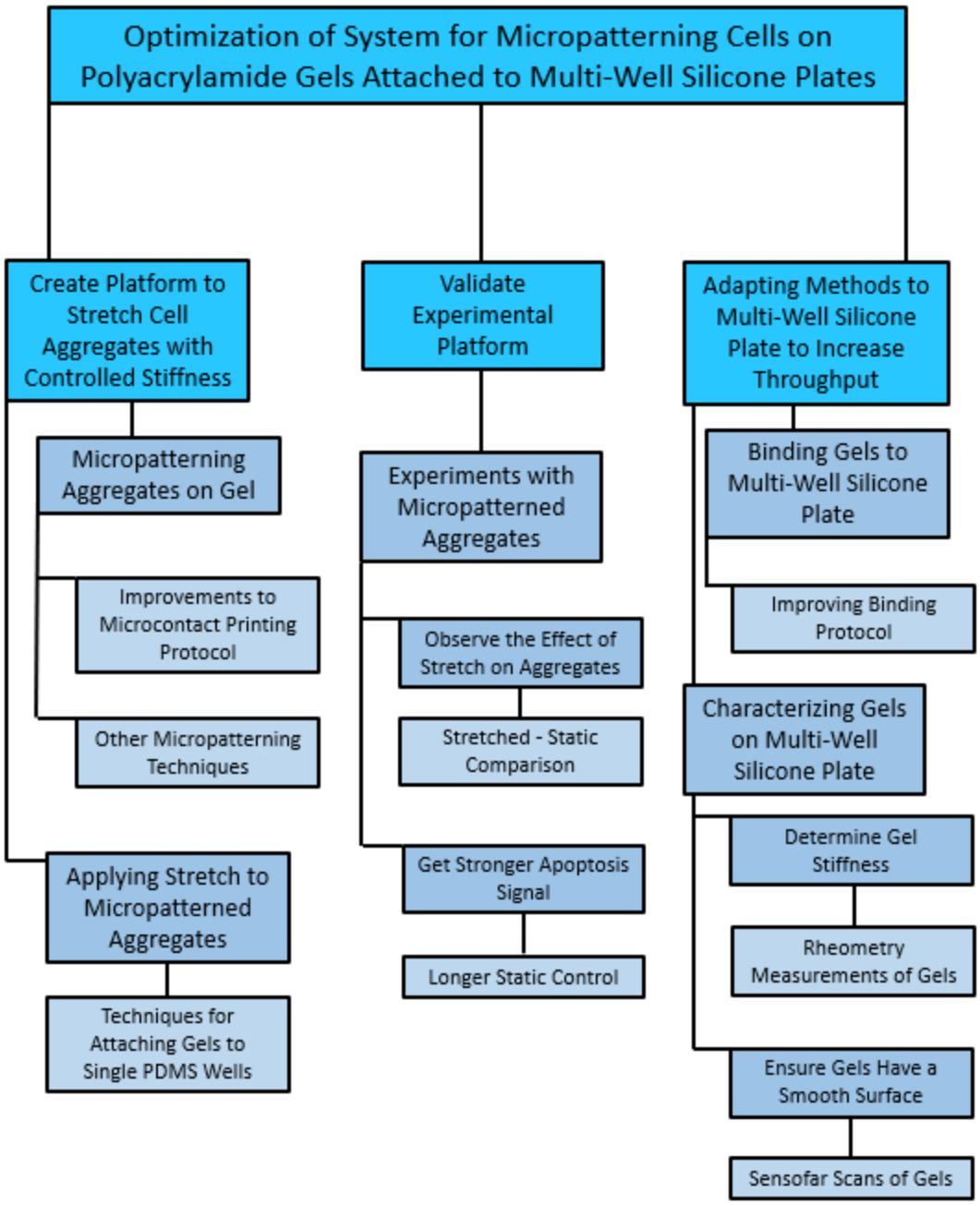

Figure 1: Project outline indicating the key elements of each part of the project.

1. Micropatterning

1.1. Background

1.1.1. Need

Micropatterning can be used to confine single cells or multicellular aggregates within a particular shape [18]. In either case, one advantage of micropatterning is the creation of many separate shapes in a single experiment, which increases throughput. Single cells can be patterned to isolate them from cell-cell contacts and to study the role of cell shape on some parameter [18]. Multicellular aggregates are used to study behaviors arising from cell-cell interactions. Aggregates create a heterogenous mechanical environment for the cells, which is useful for studying the mechanical behavior of cells in multicellular systems [6, 19].

1.1.2. History of Micropatterning

Microcontact printing is one of the earliest methods of micropatterning proteins and remains the main method. In this technique, protein is inked onto a PDMS stamp with raised features in the intended pattern, and then the stamp is brought contact with the substrate and the protein is transferred where the raised features touch the substrate. When cells can attach only to the patterned protein, the patterning of proteins enables the patterning of cells. Early microcontact printing of proteins required coating the substrates in gold, as well as certain chemicals that were not readily available [18]. Later, proteins were printed onto glass substrates. Plasma treating the PDMS stamps was required to print some proteins onto glass [18].

For certain types of studies, patterning onto substrates other than glass is necessary. In order to apply stretch to cells, cells have been micropatterned onto PDMS [6]. Some studies require softer substrates. This can be in order to determine the effect of stiffness on cell behavior [5], or because the substrates must be flexible enough that deformations caused by cells are measurable and traction force microscopy is possible [20].

Polyacrylamide and soft silicones are the most common materials used in these studies. Soft silicone materials are soft substrates that can be used as an alternative to polyacrylamide. CY52-276 is a silicone that has a tunable stiffness – both changing the ratio of the components of this material [21] or adding Sylgard-184 before curing can change its stiffness [22]. One possible advantage of silicone over polyacrylamide is that when an aggregate of cells is grown on polyacrylamide and then the substrate is stretched and released, fluid escaping the polyacrylamide can disrupt connections between the cells (so-called hydraulic facture) [15]. This is not the case with silicone [15]. There are established techniques to bind proteins to silicone. One such technique is to plasma treat the silicone, deposit a layer of APTES (3-aminopropyltriethoxysilane), bind to that a layer of glutaraldehyde, and then bind the protein to the glutaraldehyde [23, 24]. Traction force microscopy with static aggregates has been performed using silicone [25]. However, soft silicone is not used as prevalently for traction force microscopy as polyacrylamide. Polyacrylamide and soft silicones are often micropatterned with techniques other than directly microcontact printing onto them, as discussed below and shown in Figure 2.

1.1.3. Micropatterning Techniques for Soft Substrates

1.1.3.1. Direct Microcontact Printing

One way of micropatterning on a soft substrate is to microcontact print directly onto that substrate in the same manner as patterning stiff substrates. Since proteins will not adsorb onto polyacrylamide on their own, direct printing requires some chemical modification of the substrate in order to bind to the protein [26-28]. One chemical used for binding proteins to polyacrylamide gel is hydrazine hydrate. Gels are immersed in hydrazine hydrate while being modified. Hydrazine hydrate reacts with amide groups in the gel and turns them into hydrazide groups. These can bind to proteins that have been oxidized by sodium periodate [26]. Another chemical used to facilitate binding with proteins is acroyl-streptavidin. Acroyl-streptavidin is added to the gel precursor solution. The polymerized gel will then be able to bind to a biotinylated protein, which can be created by mixing a protein solution with Sulfo-NHS-LC-Biotin [27]. N-hydroxyethylacrylamide oxidized by sodium metaperiodate is an alternative that can be mixed into the precursor solution. This does not require any modification of the proteins [28]. Direct methods for printing onto soft substrates can be challenging in practice. Some of them require a dry surface, which can be a challenge with polyacrylamide [28]. Not damaging the gel by indenting it with the stamp is another potential challenge with this method.

1.1.3.2. Indirect Microcontact Printing

Another approach to micropatterning on polyacrylamide is indirect microcontact printing. In this technique, protein is microcontact printed onto a glass coverslip. Polyacrylamide is polymerized under this coverslip, and the protein transfers to the gel

[29-31]. One study found this technique to be much more effective than a direct microcontact printing technique [29]. NHS ester is sometimes incorporated into the gel in order to aid in the pattern transfer from the coverslip to the gel by binding to the protein [30]. Elevated temperature has also been used to assist with pattern transfer [31]. Not all indirect microcontact printing employs some sort of pattern transfer aid, in some cases the transfer that occurs during polymerization is sufficient [29].

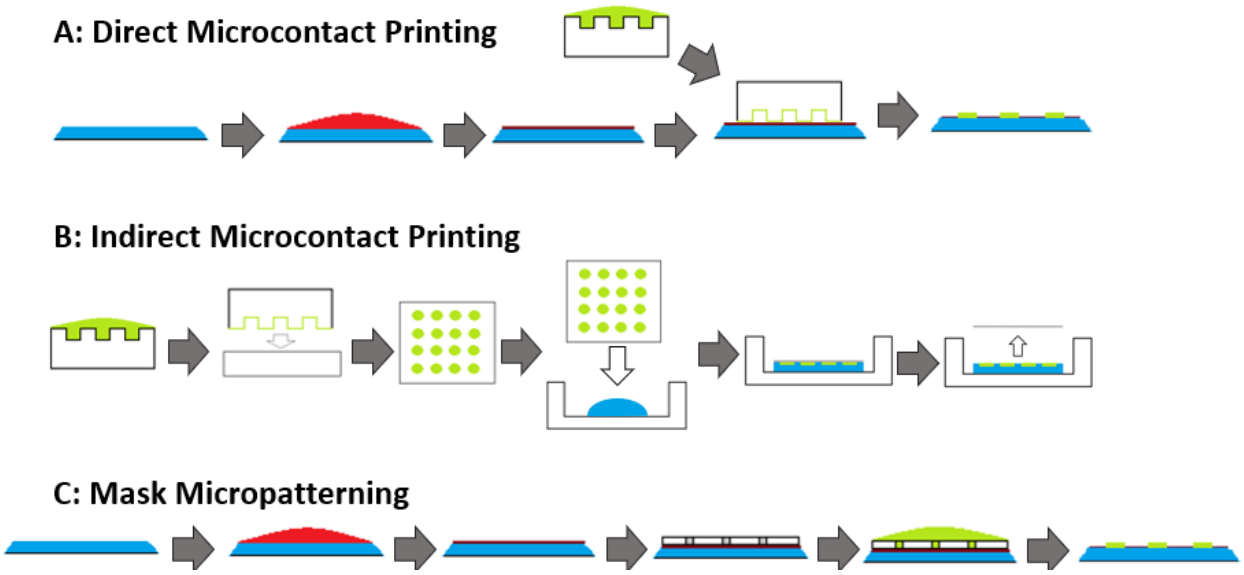

Figure 2: A,C) During direct micropatterning or mask micropatterning, the gel (blue) must be treated with some chemical such as Sulfo-SANPAH (red) to bind to the protein (green). The protein is then patterned with either a PDMS stamp or mask. B) For indirect microcontact printing, the pattern is stamped onto a coverslip and transferred onto the gel during polymerization.

1.1.3.3. Mask Micropatterning

A different approach to micropatterning is to use a PDMS membrane with holes in it. This is placed over the gel so that a fluid placed on top will only make contact with the gel where the holes are [32-34]. The membrane can be used to pattern a crosslinker, the protein [32], or both [33]. Problems can include a poor seal between the membrane and the gel and the fluid staying on top of the membrane and not entering the holes. Plasma

treating the membrane can improve the seal, and a vacuum can be applied to draw the fluid into the holes [33]. Sulfo SANPAH is commonly used to link the protein and gel [32, 33]. However, it is limited by fairly quick loss of reactivity [26]. Sulfo-LC-SDA is another crosslinker that has been used for this purpose that is not as limited in this respect [34].

Figure 3: The initial protocol for indirect microcontact printing produced ring-like patterns when confluent circles should have been produced.

1.1.4. Goal

Based on the literature, at the beginning of the project, the most promising approach for microcontact printing was indirect transfer from a coverslip. The following protocol was followed: a solution of collagen was made, leave it for an hour, plasma treat the PDMS stamps, pipette the solution onto the stamps and leave it for an hour, remove the

solution and partially dry the stamps, then stamp the coverslips in a 60 ^{o}C oven for one minute. This protocol tended to result in rings of cells when confluent circles of cells were intended, as shown in Figure 3.

Various micropatterning methods are presented in this chapter with the eventual goal of patterning in a system in which the substrate stiffness can be tuned and stretch can be applied to the micropatterned cell aggregates. Indirect microcontact printing on polyacrylamide was the main method studied, but others were also attempted. Experimental platforms combining micropatterning, tunable stiffness, stretch, and traction force microscopy are rare in literature [15, 16]. Previous work studying CAVD used static aggregates as a model [5], but the effect stretch on this model has not been studied. Here, micropatterning methods and methods to attach polyacrylamide to PDMS are attempted and evaluated for ease of implementation in our experiments.

1.2. Methods

1.2.1. Micropatterning

1.2.1.1. Microcontact Printing onto Coverslips (Final Protocol) Collagen solution was prepared from 23 μL of 4.33 mg/mL collagen (2.3% of the total solution), 77 μL 0.1 M acetic acid (7.7%), and 900 μL sodium acetate/acetic acid buffer (90%), and 1 uL Alexafluor 488 dye (0.1%, all % given as v/v). The solution was left for an hour. PDMS stamps were cleaned with ethanol and DI water. The stamps were plasma treated for 2 minutes at 100 W. Stamps had 250 μL of collagen solution pipetted onto them and were left for one hour. The stamps were dried with a nitrogen gun, then placed onto glass coverslips. The stamps were left on the coverslips for 30 minutes. The coverslips were

observed with fluorescence microscopy, only those appearing to have a good pattern were kept. New stamps were made after ~3 uses. This process is illustrated in Figure 4.

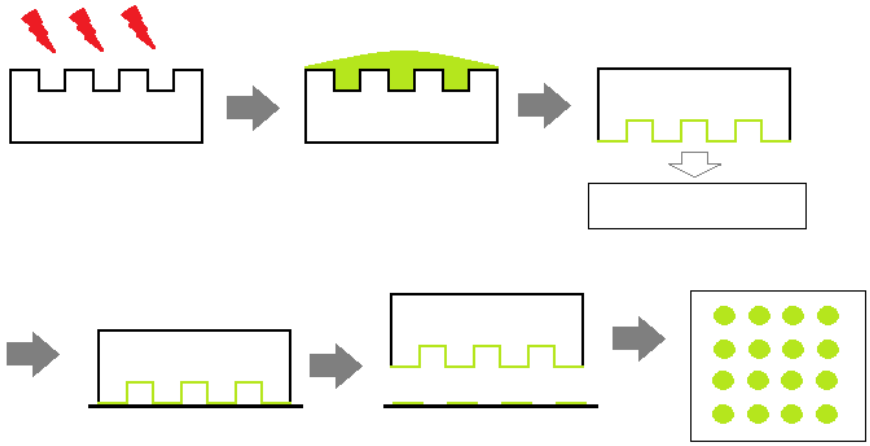

Figure 4: Illustration of the process for inking stamps will collagen. Stamps are plasma treated (red lightning bolts), then collagen solution (green) is placed on stamps. Solution is removed, coverslips are stamped.

1.2.1.2. Patterning Through PDMS Membrane

Polyacrylamide gels (standard mixture in Section 1.2.2.1) were formed on activated coverslips. A solution of sulfo SANPAH was prepared (1 % v/v sulfo SANPAH, 99% v/v HEPES buffer). ~600 µL was pipetted onto the gel, and this was placed under UV light for 15 minutes. The sulfo SANPAH solution was then aspirated off. The gel was rinsed with PBS 3 times. A plasma treated PDMS membrane with holes was placed onto the gel. A vacuum was then applied for ~3 minutes. 250 µL collagen solution (0.2 mg/mL in .02 M acetic acid) was placed on top of the membrane and left for 2 hours. The collagen solution and membrane were then removed.

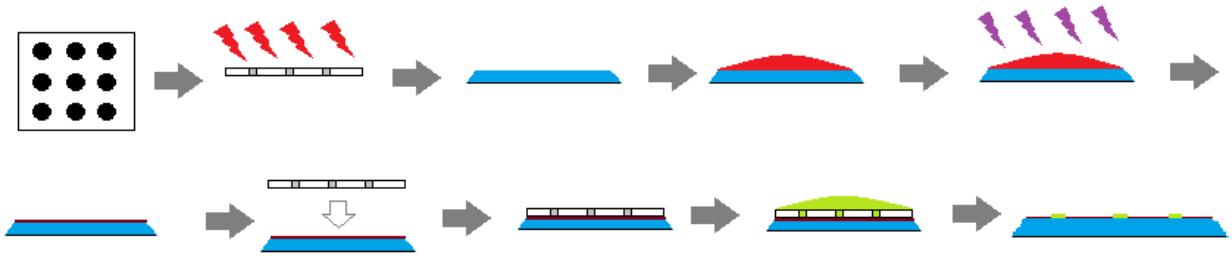

Figure 5: A PDMS membrane with holes is plasma treated (red lightning bolts). Sulfo SANPAH solution is placed on a polyacrylamide gel (blue), which is then exposed to UV light (purple lightning bolts). The membrane is placed on top of the gel, and collagen solution (green) is placed on top. The collagen binds to the gel, and then the membrane is removed.

1.2.1.3. Microcontact Printing on PDMS

PDMS stamps were coated with collagen as described in Section 1.2.1.1. PDMS wells were sonicated in ethanol for 5 minutes, then dried. The wells were plasma treated for 2 minutes at 100 W. 1 mL of APTMS was added to the wells, left for 5 minutes, and removed. 1 mL glutaraldehyde was added to the wells, left for 5 minutes, and removed. The well was then dried and stamped with collagen for 30 minutes. Bovine serum albumin in PBS was then added to prevent adsorption of other proteins from media.

1.2.2. Bind Polyacrylamide to PDMS

1.2.2.1. Binding Polyacrylamide to PDMS Using Benzophenone (Final Protocol)

NHS Ester Polyacrylamide Solution: 125 µL Acylamide, 32.5 µL Bisacrylamide, 50 µL PBS, 266.5 µL DI water, 1 µL TEMED, 35 µL 1 M HCl Solution, 6.25 µL or 3.1 µL 8 mg/mL NHS Ester Solution, 12.5 µL Ammonium Persulfate (APS)

Standard Polyacrylamide Solution: 100 µL Acrylamide, 19.6 µL Bisacrylamide, 180 µL HEPES Buffer, 1 µL TEMED, 33 µL Ammonium Persulfate

PDMS wells were sonicated in ethanol for 5 minutes, then dried. Glass coverslips were dipped in ethanol, then stuck to the bottom of the PDMS wells. While protecting from light, benzophenone solution (10 g/mL benzophenone, 35% v/v DI water, 65% v/v acetone) was pipetted into the wells covering the area where the gels would attach. The solution was left for 1 minute and the removed. Methanol was pipetted into and then removed from the wells 3 times to rinse them. The wells were then placed in a vacuum chamber and a vacuum was applied for 30 minutes (while the wells were still protected from light). The polyacrylamide precursor solution was prepared, then the wells were removed from the vacuum. Polymerization was initiated in the precursor solution, and 50 µL of polyacrylamide solution was pipetted into the center of each well. A patterned coverslip (see Section 1.2.1.1) was placed onto the polyacrylamide droplet. The wells were then left under UV light of 30 minutes while the solution polymerized. Wells were then filled with PBS, and 15 minutes later the coverslips were detached. This process is illustrated in Figure 6.

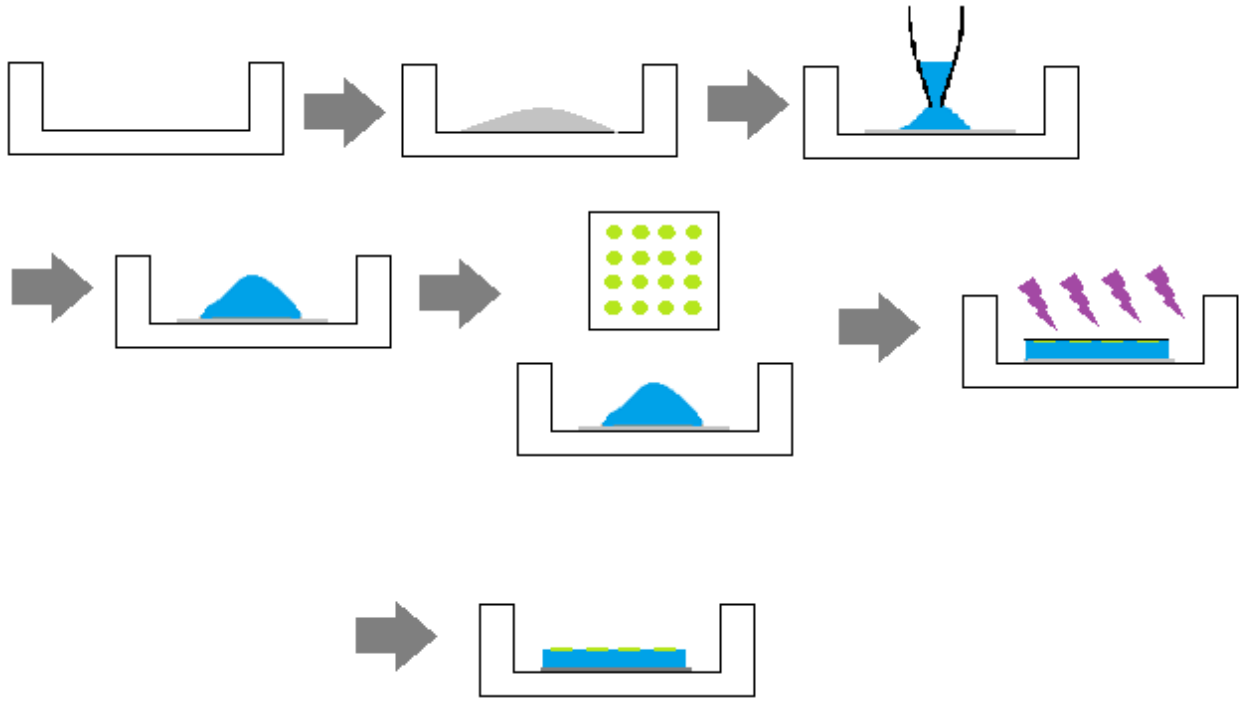

Figure 6: Benzophenone solution (gray) is placed on a PDMS well, treating the area where the polyacrylamide gel (blue) will go. The gel is pipetted in the well. The micropatterned coverslip is placed on the gel, and the well is exposed to UV light (purple lightning bolts). The coverslip is then removed, leaving behind a micropatterned gel attached to a PDMS well.

1.2.2.2. Binding Polyacrylamide to PDMS Using APTMS and Glutaraldehyde

PDMS wells were sonicated in ethanol for 5 minutes, then dried. The wells were plasma treated for 2 minutes at 100 W. 1 mL APTMS was then pipetted into the well and left for 30 minutes. The APTMS was removed, and 1 mL glutaraldehyde was pipetted into the well. This was left for 1 hour before removing. The well was dried. Polyacrylamide gels (standard mixture in Section 1.2.2.1) were polymerized between two patterned coverslips (see Section 1.2.1.1). One of the coverslips was removed, and the gel was brought into contact with the treated PDMS and they were lightly pressed together. They were then left overnight in the incubator. The following day, the remaining coverslips were removed.

1.3. Results

1.3.1. Improvements to Microcontact Printing Protocol

1.3.1.1. Stamping Parameters

Increasing the time the coverslips were stamped for from one minute to 30 minutes caused the formation of some confluent circular aggregates. The temperature was decreased to 37 ^{o}C to avoid denaturing the collagen. 37 ^{o}C in the oven was compared to an incubator at the same temperature. The incubator performed better in two experiments, but the results with the process were extremely variable and so the experiments were not conclusive. Other experiments with the microcontact printing process were performed in the oven to match as closely as possible with published protocols [31] (none of which mention increasing humidity to improve their microcontact printing process).

Experiments were conducted to see if placing a weight on the stamp while the coverslip was being stamped improved the process. No effect was observed.

1.3.1.2. Need for Fresh Stamps

It was observed that collagen solution pipetted onto the edges of new stamps tended to roll of the edges, while it tended to stay on stamps that have been used many times. This raised the possibility that repeated use would over time alter the surface properties of the stamp, which could make it less effect. It also raised the possibility the optimized parameters for newer stamps were different from those for older stamps. Going forward, only relatively new stamps (<5 uses) were used.

Table 1: The main variations of the microcontact printing protocol are summarized below. Alternative micropatterning approaches are also summarized.

Microcontact Printing				
Question	Rationale	Experiment	Result	Conclusion
What is the optimal length of time to stamp the coverslip?	Initial protocol was 1 min, but other protocols [31] have longer times	Varying time the coverslip was stamped	30 min stamping produced better results than 1 min stamping, 1 hr did not produce better results than 30 min	~30 min is the optimal stamping time.
What is the role of humidity in the stamping process?	Certain protocols [31] stamp at 37 ^{o}C, wanted to ascertain the role of humidity	Compared humid incubator to 37 ^{o}C oven	Incubator seemed slightly better, but there was too much variation in the results for that to be conclusive.	Humidity plays a small role, if any, in the stamping process.
Can weights on top of the stamp improve stamping?	Weights have been used to improve pattern transfer [31]	Weights (20 g and 50 g) on stamp while stamping	No improvement in pattern transfer	Weights on stamps are not beneficial in our stamping process.
Does freshness of stamps matter of microcontact printing?	Some protocols make new stamps each time [30].	Used new stamps instead of stamps that had been use many times	Got better pattern transfer in this and subsequent experiments	New stamps or stamps that have been used few times are better.
How does drying the stamps with nitrogen affect stamping?	Get a sense of how long should be spent drying stamps	Compared different levels of drying stamps	Intermediate level of drying got best results	Try to dry stamps a moderate amount.
Is patterning gels on PDMS different from gels on glass?	Followed goal of getting stretchable aggregates	Formed gel on benzophenone activated PDMS well [14]	Some successful patterning, but unreliable	Patterning is less effective on gels polymerized on PDMS.
Can patterning on gels before attaching to PDMS improve patterning transfer?	Thought slower polymerization on PDMS could be inhibiting pattern transfer	Formed gel on patterned coverslips and transferred to PDMS well that was activated with APTMS and glutaraldehyde [15]	Defects in the gel were often present, in these cases pattern transfer was not seen. Successful pattern transfer was not reliable even without defects in gel.	Patterning is also unreliable with this technique.

Can plasma treating coverslips before stamping improve pattern transfer?	Some protocols for microcontact printing onto coverslips include plasma treating the coverslips [30]. Rendering the surface hydrophilic could improve pattern transfer.	Plasma treated the coverslips before stamping.	The patterns seen on the plasma treated coverslips did not appear to be an improvement over those which were not plasma treated.	Plasma treating coverslips in not helpful under these circumstances.
Can additives in the gel improve pattern transfer?	NHS ester has been used to improve pattern transfer to gel [30]	Added NHS ester to gel, polymerized on benzophenone activated PDMS well	Pattern transfer did not improve, may need better control of precursor solution pH [30]	Did not help, but may be due to lack of precise pH control.
Alternatives to Microcontact Printing				
Question	Rationale	Experiment	Result	Conclusion
Can silicones be used to replace polyacrylamide?	Considering using soft silicone materials in place of polyacrylamide [21-25]	Stamped PDMS well activated with APTMS and glutaraldehyde [23, 24]	Cells attached over the whole well due to adsorption. When bovine serum albumin was used as a blocking agent, still got unpatterned cell attachment over most of the well (rings in one spot), likely due to roof collapse.	Silicones would be difficult to implement in this work.
Can patterning using a PDMS membrane with holes be used to avoid issues with indirect microcontact printing?	Potentially easier pattern transfer	Patterned sulfo SANPAH activated gel using PDMS membrane with holes [32, 33]	Leaking and bubbles were problems, but got some aggregates to form	Method shows promise, may be used in future work.

1.3.1.3. Plasma Treating Coverslips

Plasma treating the coverslips is a technique used by some to improve the transfer of protein from the stamp to the coverslip [30]. This was attempted, but it was not found to be an improvement over stamping without plasma treating.

1.3.1.4. NHS Ester

Fluorescently labeling the collagen and observing the coverslip after it has been stamped with fluorescence microscopy, it is possible to ensure the only coverslips with good patterns are used for patterning the gels. This was done, but the rate of successfully transferring good circles of collagen to the gel add thereby getting confluent circular aggregates was still low. NHS (N-hydroxysuccinimide) ester has been added to polyacrylamide gels to improve pattern transfer between coverslips and the gels [30]. NHS ester was incorporated into the gels following established protocols. However, the rate of successful pattern transfer remained low. This may be due to not having precise control of the pH of the gel precursor solution, which is recommended with NHS ester [30].

1.3.2. Other Micropatterning Techniques Attempted

1.3.2.1. Membrane with Holes

Another technique that can be used to micropattern onto polyacrylamide gel is to create a thin PDMS membrane with holes where the collagen will go [32-34]. The gel will be activated with Sulfo-SANPAH, the membrane will be placed on the gel, and the

collagen solution will be placed on top of the membrane and only make contact with and bind to the gel at the holes in the membrane.

Problems with this method can include bubbles forming in the holes in the membrane and the collagen solution leaking under the membrane. To address these issues, the membrane was plasma treated and the gel was partially dried by degassing, similar to previous protocols [33].

With this technique, some roughly circular aggregates were obtained that were 1 mm in diameter. At a diameter of .8 mm, only incomplete circles were obtained. In both cases there was some fluid leaking, as demonstrated by patches of unpatterned cell growth. The method shows promise, but still has significant barriers to implementing.

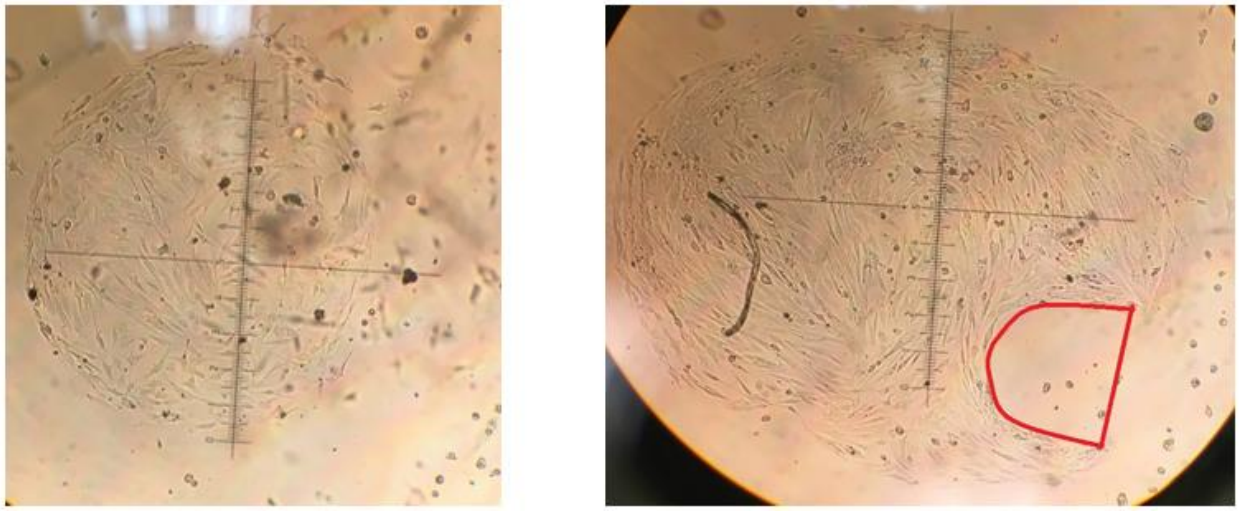

Figure 7: A PDMS membrane was created and 1 mm holes were made using a biopsy punch. A polyacrylamide gel was formed and activated with Sulfo-SANPAH. The membrane was placed onto the gel and sealed with a vacuum. Collagen solution was then placed over the membrane. After removing the membrane and remaining collagen solution, cells were seeded. The aggregate on the left appears roughly circular. The one on the left has a more oval shape, likely due to distortion of the PDMS membrane. There is also an empty patch (outlined in red) which is probably the result of a bubble.

1.3.2.2. Microcontact Printing onto PDMS

Instead of polyacrylamide gel, soft silicones can be used as a substrate with tunable stiffness. Advantages of soft silicones include not requiring any treatment to bind to the PDMS wells, and avoiding the possibility that fluid flowing into or out of the substrate would affect the cyclic stretch experiments [15]. Stamping onto the PDMS wells was attempted to test the method before moving to a softer silicone. To facilitated collagen binding to the PDMS, the wells were treated with APTMS and glutaraldehyde in the same manner as the CellScale silicone plates. The wells were then stamped directly. When cells were seeded, the cells grew everywhere, not just where the collagen was patterned. This is believed to be due to proteins from the media attaching to the PDMS. To prevent this, the wells were coated with BSA (bovine serum albumin), which can be used to block unwanted protein attachment [35]. Despite this, there was still unpatterned cell growth. However, there was a small region in which the cells only grew in rings (of the type seen where microcontact printing has not been successful). This could be explained by the roof of the stamp making contact with the substrate over all but a small area.

1.3.3. Techniques for Attaching Gels

There are two ways that have been used for attaching polyacrylamide gels to the larger PDMS wells. One is to bind the gel to the PDMS using benzophenone [14]. The PDMS is activated with benzophenone, rinsed with methanol, and then degassed for 30 minutes. A drop of polymerizing gel is then place on the PDMS and a coverslip is place on top. The gel is then left to polymerize under UV light for 30 minutes. Experiments described in Section 2 are performed using this technique.

Another technique is to attach the gels to the PDMS using APTMS and glutaraldehyde. The PDMS is plasma treated, then treated with APTMS and glutaraldehyde. In this technique, the gels are made beforehand between two glass coverslips. One of the coverslips is then removed, and the gel is then placed in contact with the treated PDMS. It is left overnight in the incubator, and then the remaining coverslip is removed [15]. This technique was attempted to see if polymerizing between two glass coverslips would improve pattern transfer and to explore methods that did not require the use of UV light, which will photobleach fluorescent dyes.

1.4. Discussion

The goal of this portion of the project was to develop a technique to micropattern cell aggregates onto polyacrylamide gels attached to PDMS. The technique arrived at during the project performed this function. However, it did not do so reliably. Even after optimization, the percentage of gels which will have aggregates on them is low (25%, n=16), and number of aggregates on the gel is much lower than the number of collagen circles patterned. Since this problem persists even when the pattern is shown by fluorescent labeling to have transferred to the coverslip, the problem must be the transfer of the collagen from the coverslip to the gel. NHS Ester added to the was not effective in improving pattern transfer, but this may be due to a lack of control over the pH of the precursor solution [30]. Future experiments measuring the pH of the precursor solution and precisely adjusting it may improve results.

The other technique which shows promise is micropatterning using a PDMS membrane with holes where the collagen will go. Preliminary investigation with this technique did obtain some

aggregates. It is likely that the technique can be made reliable by adjusting the details of the procedure. However, going from the larger single PDMS wells to the smaller wells of the CellScale silicone plate may be more of a challenge with this technique. A small PDMS membrane would be difficult to manipulate and place properly within a small CellScale well. Techniques besides the two mentioned did not show a strong potential for successful use in the context of this project.

In summary, a technique to micropattern polyacrylamide gels on PDMS wells is developed, albeit with significant limitations. Going forward, indirect microcontact printing on gels bound to PDMS wells with benzophenone will be used. Several patterning attempts will be made, and those that successfully form aggregates will be used for experiments.

2. Experiments with Aggregates

2.1. Background

The process of calcification in calcific aortic valve disease is known to be regulated by mechanical factors. It has been shown that valvular interstitial cells exhibit increased calcification in response to elevated strains [2], which has also been shown in heart valve cusps [3]. Calcification be caused either by osteogenesis or by apoptosis. Cells grown on very stiff substrates (with elastic moduli of 110 kPa) such as glass or plastic tend to calcify by apoptosis, whereas cells grow on less stiff substrates (with elastic moduli of 25 kPa) tend to calcify by osteogenesis [36].

Previous work in our group studied calcification and apoptosis in circular aggregates of cells. It was found that the cells in the center of the aggregates exhibited more calcification

and apoptosis than peripheral cells, and that there were smaller traction stresses on the cells in the center [5]. This raised the possibility that the lower stress state of these cells was responsible for the apoptosis and calcification. One way to test this is to raise the stress state in the center of the aggregates, which can be done using cyclic stretch [6]. So far, no work has studied the effect of cyclic stretch on apoptosis or calcification in aggregates.

In addition to calcification and apoptosis, cell alignment is also likely to be affected by cyclic stretch. A major way cells react to the application of cyclic stretch is realigning themselves. Cells tend to align perpendicular to the direction of stretch in cells on a 2D substrate [8]. Being confined in an aggregate can also significantly influence cell alignment [37, 38]. The role of cyclic stretch on alignments in aggregates is not understood.

Previous work has looked at the effect of stretch and release on stresses in aggregates [15, 39]. Other work created a thermal contraction model based on measuring traction forces on static aggregates and used it to model the effect of cyclic stretch, but was not able to measure traction forces on the cyclically stretched aggregates [6]. There has not been a measurement of the traction forces exerted by cyclically stretched aggregates. Here, aggregates are patterned onto polyacrylamide (which gives the potential for TFM if beads are added) attached to PDMS in order to enable cyclic stretching. Apoptosis is measured in static and cyclically stretched aggregates.

2.2. Methods

Polyacrylamide gels (18 mm square gels) were attached to PDMS wells and 400 μm diameter circular aggregates were micropatterned as described in Sections 1.2.1.1 and 1.2.2.1. Porcine

valvular interstitial cells were seeded into each well (125,000 per well). Stretched wells were strained 10% uniaxially at 1 Hz overnight with a custom stretching device. Before imaging, aggregates were stained with Caspase and Hoechst.

ImageJ was used to determine the area positive for caspase. First, the background was subtracted. An intensity threshold was then manually set which clearly differentiated caspase signal from remaining background noise. The area where the intensity of the caspase signal was above this threshold was found and divided by the area of the aggregate to compute the percent area positive for caspase, as illustrated in Figure 8. At least 3 connected pixels were required to be part of the caspase positive area in order to further reduce noise.

The alignment of the nuclei was also found using ImageJ. The nuclei were found using thresholding of the Hoechst images and the Watershed feature. The alignment and coordinates of each nuclei could then be found using the Analyze particles feature. The coordinates of the center of each aggregate, found by manually outlining the aggregate with an ellipse, were also recorded. Further analysis of the alignment with respect to different directions (x, y, r, θ) was then carried out in MATLAB.

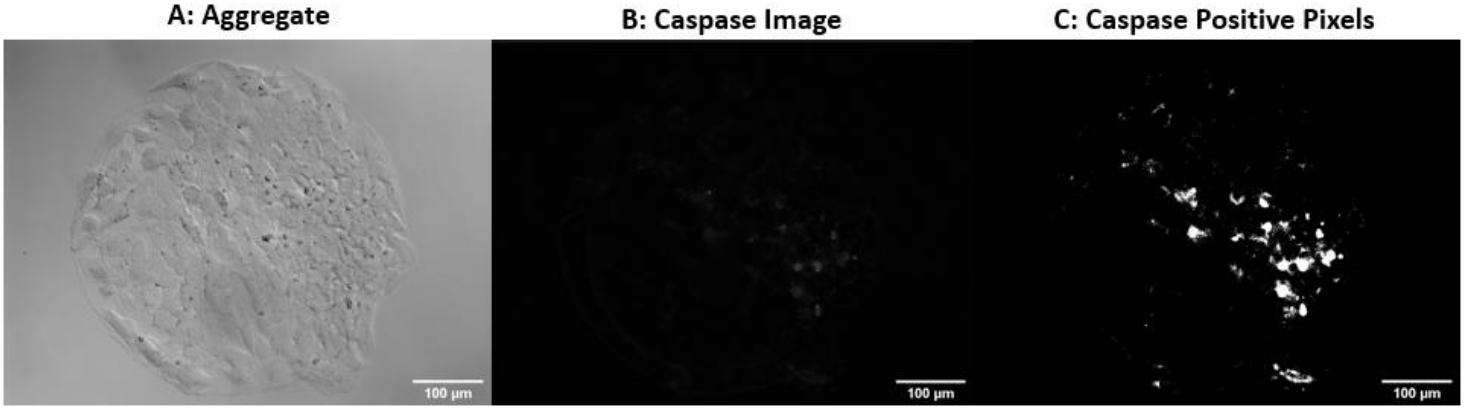

Figure 8: Representative images of the process of the process for analyzing the aggregates for apoptosis. A) An aggregate. B) The raw caspase image of the aggregate. C) The pixels found to be positive for caspase by subtracting the background and setting a threshold are shown.

2.3. Results

2.3.1. Stretched and Static Aggregates

Aggregates in two wells (with gels made from the standard polyacrylamide solution described in Section 1.2.2.1) were cultured for 3 days, with one being cyclically stretched overnight for the last night of culture. The wells were then stained with Caspase and Hoechst. Area undergoing apoptosis in the stretched and static wells was compared, but the difference was not statistically significant. In both cases the area was small: 2.5% ± 1.4% for static, 2.3% ± 1.6% for stretched (Figure 9).

2.3.2. Longer Static Control

Aggregates were cultured for 5 days on gels made from the NHS ester polyacrylamide solution described in Section 1.2.2.1. Apoptosis increased to 9.5% ± 5.5%, significantly greater than the aggregates cultured for 3 days (Figure 9). The alignments of the nuclei were also analyzed. There was not found to be significant radial or circumferential alignment in these aggregates (Figure 10).

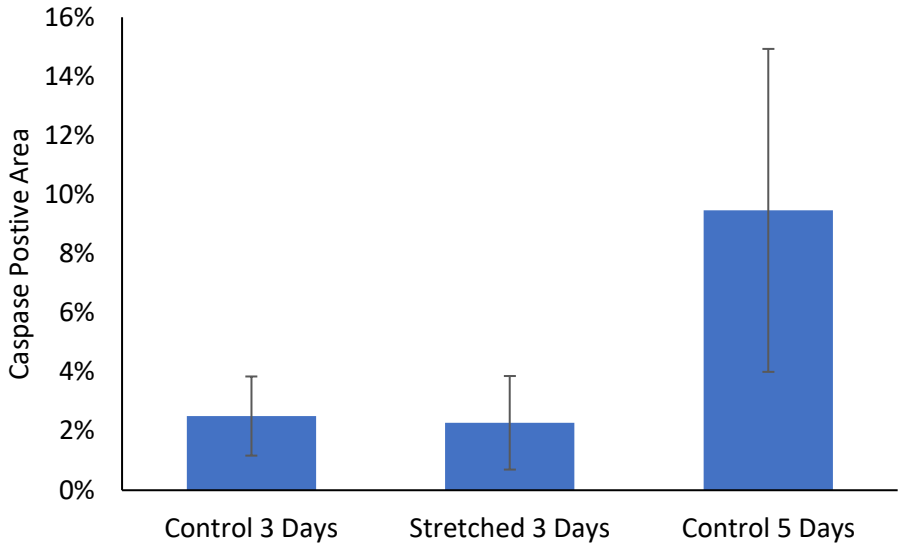

Figure 9: Apoptosis in different aggregates under different conditions (static control or stretched cyclically overnight). At 3 days in culture, little apoptosis occurred in either control or stretched aggregates. Increasing the culture time to 5 days increases apoptosis in control aggregates. n=9,11,10 respectively. Error bars indicate standard deviation.

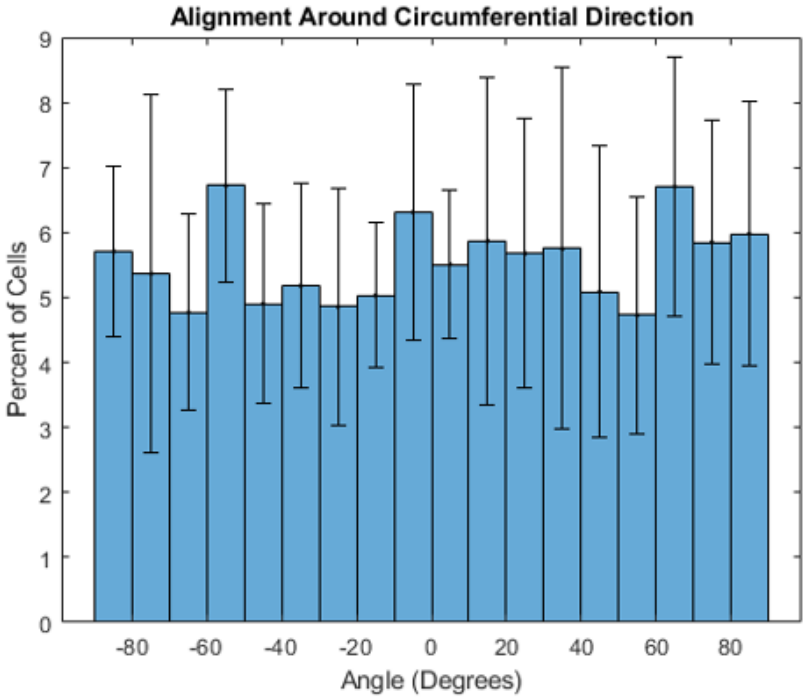

Figure 10: Analysis of the alignment of cell nuclei in aggregates cultured for 5 days. Error bars indicate standard deviation, n=10 aggregates. Angles are measure from the circumferential (counterclockwise) direction, and those angles sweeping outward from the aggregate are positive.

2.4. Discussion

Aggregates of cells (sometimes referred to as cell islands) are known to produce heterogeneous mechanical forces on their surroundings and non-uniform stresses between the cells that comprise them. This has been shown in previous work using traction force microscopy (TFM), a technique in which the traction forces the aggregates exert on their substrate are calculated by measuring the displacements of beads within the substrate of known elastic modulus [20], traction forces are generally shown to be higher around the outer portion of the aggregate and negligible in the central region [5, 8, 15]. But TFM only calculates stress on the surface of the substrate, not within the monolayer of cells itself. There are a few different approaches that have been used in previous work to calculate stresses within the cell layer using TFM data [6, 40, 41].

For computing stresses within a 2D cell layer from traction force microscopy data, monolayer stress microscopy (MSM) was developed. The stresses are computed by calculating the forces on the aggregate that are required to balance out the tractions on the substrate using a finite element method [41]. Assuming uniform mechanical properties throughout the aggregate, this technique yields higher stresses on the interior cells than the outer cells even though the measured tractions are higher in the outer region [19]. The stresses calculated from MSM are anisotropic with higher stresses in the circumferential direction as opposed to the radial direction towards the edge of an aggregate, but similar stresses in each direction toward the center [19].

Stresses within an aggregate have also been estimated using thermal contraction models and vertex models. Thermal contraction models treat the aggregate as a material bound to the substrate, “cool” the aggregate (similar to applying a uniform prestrain), and observe the

stresses as a result of the cooling. By comparing stresses on the substrate estimated using this model to the stresses calculated from traction force microscopy, an effective temperature drop can be found and used to estimate stresses on the aggregate [6]. Thermal contraction models generally show the same trends as monolayer stress microscopy of uniform properties (coefficient of thermal expansion and elastic modulus) are assumed, with the stress being higher in the center of the aggregates [19]. Vertex models model each cell as elastically deformable polygons. An energy based on the state of these polygons is calculated, and the vertices of the polygons are positioned in a manner which minimizes this energy. Recently, vertex models have been used to model the intercellular stress in aggregates, also finding higher cell-cell stresses in the inner region of the aggregate [40]. The vertex model also assumes homogeneous elastic modulus for each cell.

In contrast to the model predications and calculations, markers of high stress in cells in these aggregates are higher on the outside of the aggregates, following the traction stress patterns [6]. This indicates that either the modeling discussed above does not match reality or that cell-substrate interactions dominate cell-cell interactions. New work by our group has incorporated heterogeneity in cell mechanical properties (which differ between the edge and the center of the aggregate) and calculated higher stresses in the edges of the aggregates [19]. This result is in agreement with the aforementioned markers of high stress [6].

The anisotropic stresses and heterogeneous mechanical environment above are expected to produce cell alignment within the aggregates. Alignment within aggregates has been observed previously [37, 38]. However, no such alignment was observed here visually or through image analysis. This may be due to a short time spent post confluence. The 3 day culture time for early trials was chosen because that was when the aggregates seen to be

confluent were confluent, leaving ~2 days for the cells to interact and develop alignments while confluent. It is possible that longer time is require for alignment patterns to emerge in these aggregates.

The goal of this portion of the project was to validate this experimental platform. Here, the successful creation and stretching of aggregates is shown. It was found that aggregates must be cultured for at least 5 days in order to undergo enough apoptosis for a reliable comparison of apoptosis levels in stretched and unstretched aggregates. The analysis approach for determining the levels of apoptosis in aggregates is demonstrated. An approach for observing alignment in aggregates are also demonstrated, but alignment is not seen in the aggregates.

3. Gels on CellScale

3.1. Background

Tunable stiffness polyacrylamide gels are commonly used in mechanobiology to study the effect of stiffness on some cell behavior. They are also commonly used for traction force microscopy (TFM), a technique by which the forces exerted by cells grown on polyacrylamide gels can be measured by observing the displacements they cause on beads embedded within gels of known stiffness [42]. More recently, polyacrylamide gels are being bound to PDMS substrates in order to make them stretchable [14, 15]. These techniques tend to only enable the stretching of one gel at a time, a higher throughput system would be beneficial. The CellScale MCFX is a commercially available uniaxial stretch device which can stretch a silicone plate with 16 wells, dramatically increasing throughput [17]. The silicone plate required developing a new method to bind the polyacrylamide gel to it. Once

the new method was developed, the gels needed to be characterized to determine their storage modulus and if they were smooth enough for experiments.

Polyacrylamide gel is made from polymerizing acrylamide and bisacrylamide in water or a buffer solution. Ammonium persulfate (APS) polymerizes the components by contributing free radicals, and TEMED is used to accelerate this process. This process is inhibited by oxygen. Notably, the concentrations of APS and TEMED can affect the mechanical properties of the gel, with higher concentrations leading to longer chain lengths and therefore less stiff gels [43]. However, the concentrations of acrylamide and bisacrylamide are the main parameters used to tune the gel stiffness [44].

A common approach to binding polyacrylamide to glass is by using APTMS ((3-aminopropyl) trimethoxysilane) and glutaraldehyde. In this technique, a layer of APTMS is bound to the glass, a layer of glutaraldehyde is attached to the glass, and the glutaraldehyde binds to the polyacrylamide gel [45]. Treating PDMS in a similar fashion has been used to bind polyacrylamide gels to PDMS, except the when binding to PDMS in this manner the gels were polymerized beforehand and then transferred to the PDMS [15]. The main alternative for binding polyacrylamide to PDMS is the use of benzophenone. Benzophenone is deposited onto the PDMS, and then polymerizing gel is placed on top. Binding is facilitated by exposure to UV light [14]. The benzophenone technique is quicker than the APTMS and glutaraldehyde approach as described above, but the UV light it uses could photobleach fluorescent dyes used in labeling proteins.

A variety of techniques have been used to measure the stiffness of polyacrylamide gels. These techniques include AFM, micropipette aspiration, stretching, microindentation, compression, dynamic light scattering, and rheometry [44]. Notably, mechanical

measurements of viscoelastic materials used in mechanobiology studies can vary significantly depending on the measuring technique. This has been found to be the case with PDMS [12] and polyacrylamide [44]. Rheometry is commonly used to characterize the stiffness of the gels. Rheometry involves polymerizing the gel between two plates, one of which oscillates at a programmed amplitude and frequency. The device records the shear stress and then calculates the storage modulus G' and loss modulus G''[46].

Surface roughness can have a variety of effects on cell behaviors. It can influence cell attachment, spreading, proliferation and differentiation. Different studies sometimes find contradictory roughness based effects [47]. Therefore for our experiments, it is desirable to minimize roughness in order to avoid roughness effects interfering with studying the parameters of interest. It was unclear if the different polymerization conditions caused by changing substrate and binding protocols would affect surface roughness.

Here, optimization of a procedure to bind polyacrylamide gel to the CellScale silicone plate is described. The procedure as previously developed consisted of cleaning and plasma treating the silicone plate, placing APTMS into the wells for 5 minutes, removing it and placing glutaraldehyde into the wells for 5 minutes. This creates a surface which can bind to the polyacrylamide gel. Polymerization was then initiated in the gel precursor solution, and droplets of the polymerizing solution were placed into the wells. 5 mm circular coverslips were then immediately placed on top of the droplets. The silicone plates were then placed into a vacuum chamber and degassed to avoid the presence of oxygen, which interferes with the polymerization [43]. After degassing, the chamber was filled with nitrogen. The gel was left to polymerize 45 minutes in the case of a stiffer gel and 1.5 hours in the case of a softer

gel. After removing from the vacuum chamber, DI water was added to the wells to loosen the coverslips. Shortly after (~1 minute), the coverslips were removed.

The procedure described above frequently produced gels which were in the shape of rings, instead of the desired disk-shaped gel. Gels would also sometimes be found to have a surface which was visibly rough.

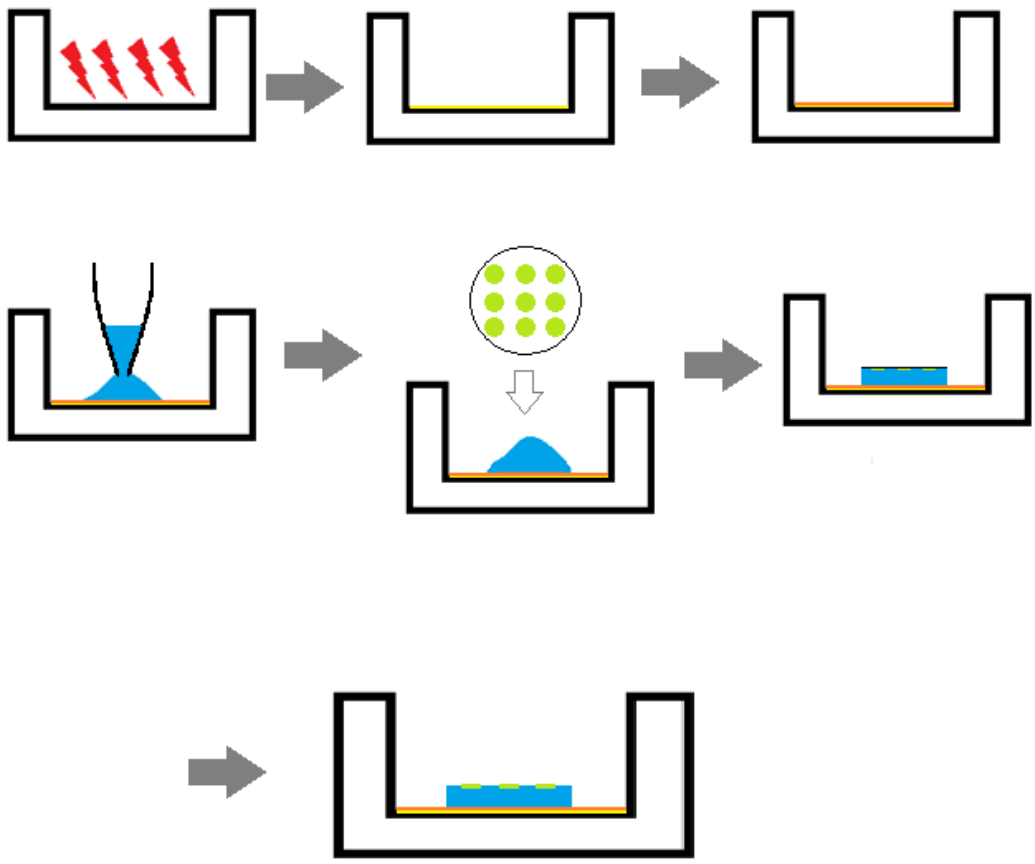

Figure 11: Illustration of the protocol for binding polyacrylamide gel to the CellScale silicone plate. First the silicone is plasma treated (red lightning bolts). Next, a monolayer of APTMS is deposited (yellow). A monolayer of glutaraldehyde (orange) is then deposited on top of the APTMS layer. A droplet of polyacrylamide precursor solution (blue) is placed on the treated surface, and a coverslip with a collagen pattern (green) is place on top while the solution polymerizes. Once the solution is done polymerizing, the coverslip is removed and the collagen pattern is transferred to the gel.

3.2. Methods

Initial Protocol for Binding Polyacrylamide Gels to CellScale Silicone Plate

The following procedure was previously developed in our lab to bind polyacrylamide gels to the CellScale silicone plate. A gel precursor solution was mixed (for stiff gels 100 µL 40% Acrylamide, 19.6 µL 2% Bisacrylamide, 180 µL HEPES Buffer, 1 µL TEMED, for soft gels: 25 µL 40% Acrylamide, 17.9 µL 2% Bisacrylamide, 257 µL HEPES Buffer, 1 µL TEMED). The plate was plasma treated for 2 minutes at 100 W. Next 100 µL 1% APTMS ((3-aminopropyl) trimethoxysilane) was pipetted into wells, left for 5 minutes, then removed. Then 100 µL .5% Glutaraldehyde was pipetted into wells, left for 5 minutes, then removed. To initiate polymerization, 33 µL 1% APS (Ammonium Persulfate) was added to precursor solution. A 2.5 µL droplet of polymerizing gel solution was pipetted into each well being used. A 5 mm coverslip was placed on each droplet. The silicone plate was placed in a vacuum chamber, vacuum was applied for 30-45 seconds. The chamber was refilled with nitrogen, and the gels were given time to polymerize (45 minutes for stiff gels, 1.5 hours for soft gels). Gels were soaked in DI water for a few minutes, then the coverslips were removed.

Final Protocol for Binding Polyacrylamide Gels to CellScale Silicone Plate

A gel precursor solution was mixed (for stiff gels 100 µL 40% Acrylamide, 19.6 µL 2% Bisacrylamide, 180 µL HEPES Buffer, 1 µL TEMED, for soft gels: 25 µL 40% Acrylamide, 17.9 µL 2% Bisacrylamide, 257 µL HEPES Buffer, 1 µL TEMED). The plate was plasma treated for 2 minutes at 100 W. Next 100 µL 1% APTMS ((3-aminopropyl) trimethoxysilane) was pipetted into wells, left for 5 minutes, then removed. Then 100 µL .5% Glutaraldehyde was

pipetted into wells, left for 5 minutes, then removed. To initiate polymerization, 33 µL 1% APS (Ammonium Persulfate) was added to precursor solution. A 4 µL droplet of polymerizing gel solution was pipetted into each well being used. A 5 mm coverslip was placed on each droplet. The silicone plate was placed in a vacuum chamber nitrogen was flowed through the tank for 1 minute. The gels were given time to polymerize (45 minutes for stiff gels, 1.5 hours for soft gels). Gels were soaked in DI water (30 minutes for stiff gels, 1 hour for soft gels), then the coverslips were removed.

3.3. Results

3.3.1. Improving Binding Protocol

Table 2: These are some of the main modifications to the protocol for binding polyacrylamide gels to the silicone plates and their results. The most significant modifications are discussed more in Sections 3.3.1.1 and 3.3.1.2 .

Question	Rationale	Modification to Protocol	Result	Conclusion
Does the volume influence the successful formation of gels?	A gel with more volume may be less prone to forming rings, smooth due to less effect from silicone surface.	Increased volume from A: 2.5 µL to B: 3 µL	A: 70% rings, 20% rough partial gels, 10% rough fully formed gel (n=10) B: 70% rings, 20% proper gels, 10% rough gels (n=10)	Increased volume improved gel formation.
Can pipetting by capillary action improve gel formation?	Placing the coverslips might push the gel into a ring or create a rough surface.	Placed coverslips beforehand with a gap created by other coverslips or wire.	Gels were drawn around whatever was holding up the coverslip and did not form properly (n=6).	Pipetting by capillary action is not feasible in this system.
Does refilling the vacuum chamber with nitrogen affect gel formation?	Turbulence during refilling might affect gels during polymerization.	Timed vacuum for 15 s, did not refill chamber with nitrogen	50% rings, 20% partially formed gels, 20% rough gels, 10% properly formed gels (n=10)	Refilling with nitrogen is not responsible for gel defects.
Is will oxygen interfere with polymerization under these conditions? Does the vacuum cause the gel defects	Oxygen is known to inhibit polymerization, but polymerization is still often conducted in normal air. Vacuum could be responsible for drawing gels into rings.	Polymerized gels outside vacuum chamber in normal air	Gels did not form (n=2)	Gels must be protected from oxygen to form.

Does applying vacuum cause defects?	Vacuum could draw gels into rings.	Flowed nitrogen through the vacuum chamber for 60 s to removed oxygen instead of using the vacuum	Gels formed properly (n=6)	Vacuum was responsible for ring problem.
Will applying a hydrophobic coating smooth the gel surfaces?	Gels may be partially sticking to coverslip.	Applied Rain-X to coverslip to see of it resulted in a smoother surface	Surface did not improve (n=2)	Hydrophobic coatings are not an effective way to prevent rough gels.
Will further increasing the volume reduce gel roughness?	Gels with more volume may be less affected by roughness on the bottom surface.	Increased volume to 4 µL	Surface was smoother (n=4)	Increased volume decreases roughness.
Will longer times spent under DI water after polymerization improve the formation of intact gels with smooth surfaces? Will twisting off the coverslips accomplish the same?	Gels may be partially sticking to coverslip, and DI water has been shown to loosen them. Twisting off might also reduce sticking.	For soft gels: Tried 30 min in DI water and twisting off coverslip, 1 hr in DI water and lifting off coverslip, and 1 hr in DI water and twisting off coverslip For stiff gels: Increased time in DI water to 30 min and twisted off coverslips	For soft gels: 30 min in DI water and twisting off coverslips produced 1 smooth gel and 1 ring (n=2) 1 hr in DI water and lifting off coverslips produced rings (n=2) 1hr in DI water and twisting off coverslips gave smooth gels 77% of the time (n=13) For stiff gels: 30 minutes in DI water and twisting off coverslips improved rate of smooth gel formation to 75% (n=8)	1 hr in DI water and twisting off coverslips is required to produce smooth soft gels, 30 min in DI water and twisting off coverslips is sufficient for stiff gels

3.3.1.1. Vacuum

It was found that when, instead of degassing, nitrogen was flowed through the vacuum chamber for one minute and then the chamber was closed, the gels no longer formed rings. This indicated that the degassing had been drawing the gel into rings.

3.3.1.2. Time in Water Before Removing Coverslips

Roughness and other defects in the gels was believed to be caused by gel sticking to the coverslips as they were removed. Increasing the time in which the gel soaked in water to 30 minutes for stiff gels was found to greatly reduce this problem for stiff gels. 30 minutes was not sufficient for soft gels, but one hour of soaking was found to significantly reduce the defects in soft gels as well.

3.3.2. Rheometry Measurements of Gels

It was hypothesized that the different conditions under which the polyacrylamide gels polymerized in our process could affect the stiffness of the gel. Therefore, a rheometer (Anton-Paar MCR 302 WESP) was used to characterize the storage modulus of the gels.

3.3.2.1. Gelation Tests

Gelation tests consisted of initiating polymerization in a polyacrylamide precursor solution, pipetting the solution onto a glass plate (part of the rheometer), and bringing down the top plate of the rheometer. The plate would then oscillate at a programmed amplitude and frequency as the gel polymerized while recording the normal force, shear stress, and torque and calculated the storage modulus and loss modulus from that data. Results of these tests are shown in Figure 12.

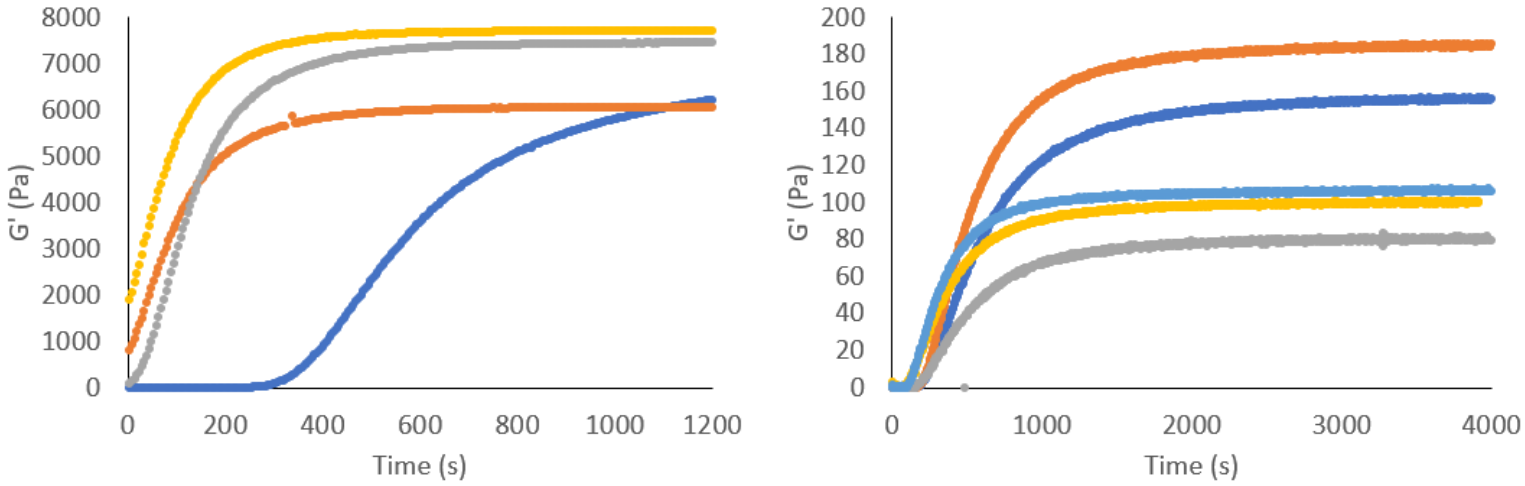

Figure 12: Gelation tests for the stiff gels (left) and soft gels (right). Polymerization is initiated in gel precursor solution, and then the rheometer's 25 mm plate is lowered onto the solution. Stiff gels polymerize significantly faster than soft gels, so the tests are run for different lengths of time. It is not clear why one of the stiff gels was slower to polymerize than the others, it may be the test was started sooner after polymerization was initiated with this sample. Longer testing showed the G' for this sample leveling off (data not shown).

3.3.2.2. Rheometry of Gels on CellScale

Measuring gels made on the CellScale silicone plates involves complications not seen in the gelation tests. First, initial measurements of the gels were extremely inconsistent between them. It was also found that the storage modulus measured for a single gel would vary significantly over time. It was hypothesized that this was due to the gel drying out. To keep the gel hydrated, DI water was placed in the corners of the well, and a paper cover was placed on the well and then wet with DI water. This stabilized the measurements from the gels.

Despite the gels being properly hydrated, there was still the possibility that the gel would not be properly aligned with the rheometer's measurement tool. Visual alignment was difficult while the gels were in the CellScale wells. Therefore, the bottom of the

wells (to which the gels were attached) was cut out. This made visual alignment easier, and it allowed the solvent trap, used to contain samples and help keep them hydrated when water is added within, to be used. Previously the solvent trap could not be used because the CellScale silicone plate would not fit inside.

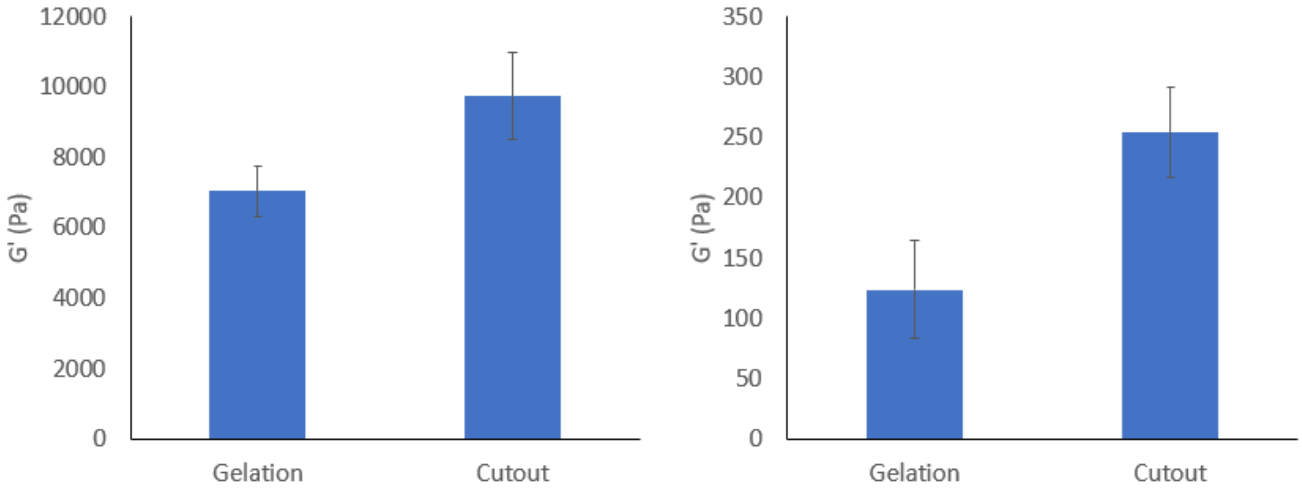

Figure 13: The storage modulus of different gel formulations, with higher modulus gels on the left and lower modulus gels on the right (referred to elsewhere as stiff gels and soft gels), polymerized under different conditions - either on the glass base of the rheometer (gelation) or on the CellScale silicone plate (cutout, because the base of the wells with the attached gel were cut out from the plate). Error bars indicate standard deviation.

Noise was also investigated as a possible source of variation in the measured storage moduli. In order to account for this, a Fast Fourier Transform (FFT) of the data was taken. Significant noise was seen. The signal at the frequency at which the gel was strained was compared to the minimum from the manufacturer specifications. It was determined that for soft gels, very small strains such as 0.1% did not produce reliable data, but 2% strain was sufficient to produce reliable data. The storage modulus was calculated using the value of shear stress the frequency at which the gels were strained and compared to the data from the rheometer. There was good agreement, indicating that the rheometer was filtering the noise properly on its own. The loss modulus was also measured, this is shown in Figure 15 in Appendix 3.

3.3.3. Sensofar Scans of Gels

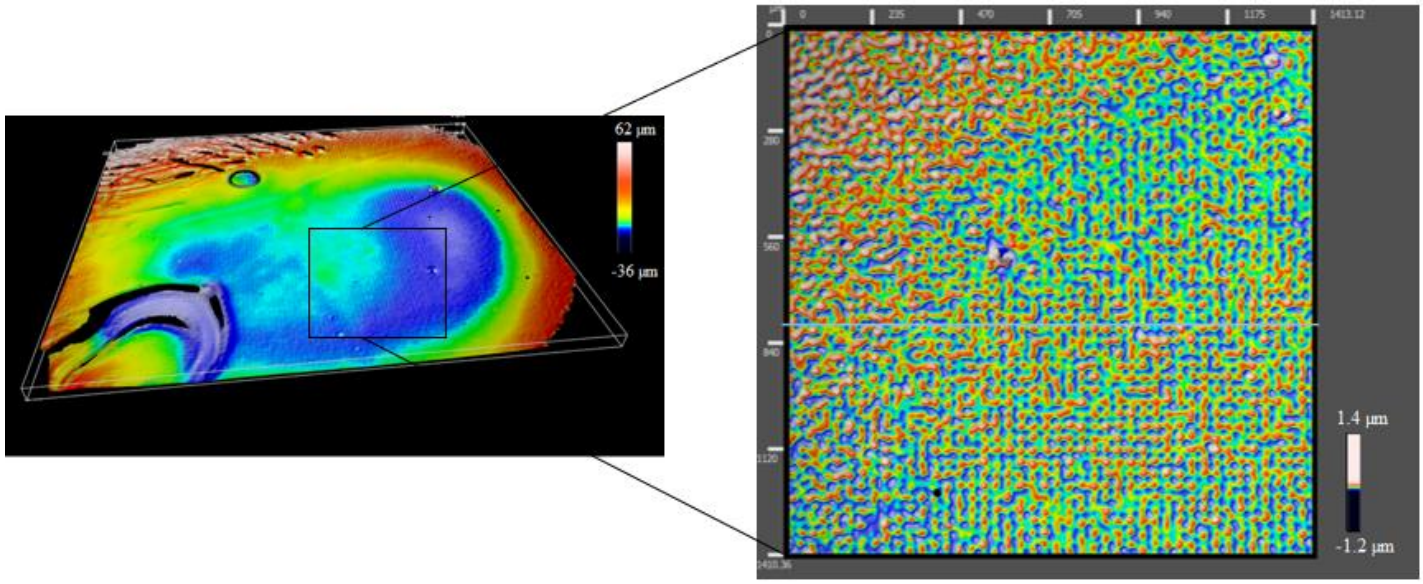

Figure 14: Surface scans of a gel made on a CellScale silicone plate. The gel is approximately 5 mm across. Gel surface (left) and filtered center surface (right) indicating roughness on length scales below 25 microns, corresponding to roughness that cells would be able to detect. The gel surface appears smooth in the center, so roughness affecting experiments for cells or aggregates not near the edge is unlikely. This is confirmed with the filtered image, with roughness mainly on the sub-micron scale.

In order to characterize the surface of the gels, scans of the surface (Figure 14) were taken using a Sensofar S Neox microscope. The scans were filtered so that only roughness at lengths below 25 µm would be included, since slopes over longer length scales would not be noticeable to cells. The gels on the CellScale silicone plate were found to be acceptably smooth (although not as smooth as control gel on a glass coverslip). The scans show that care must be taken to avoid using cells or aggregates near the edge in analysis, but the central region of the gel is usable. It was found that the gels on the silicone plate had an average filtered roughness of $S_a = 68 \pm 58$ nm, S_a being a measure of the average distance from a point and the average height. It was decided that this value was smooth enough for these experiments. A gel polymerized on glass had an S_a of 13 nm.

3.4. Discussion

Here, a method which reliably binds polyacrylamide gels to CellScale silicone plates is described. The gels were found to have surfaces that are smooth enough for experiments. The stiffness of the gels is characterized by their storage modulus. The key points to successfully forming and binding gels were found to be avoiding using a vacuum during polymerization and soaking gels for long time periods after polymerization.

Polyacrylamide gels polymerize much faster on glass than on silicone. This can be seen by comparing the time it takes to polymerize in the protocol for binding to the silicone plate to how long it takes for the G' curves in the gelation tests to level off. By comparing the gelation tests where gels were formed on glass to the tests of the gels formed on the silicone plate (see Figure 13), it can be seen that the gels formed on glass have a lower storage moduli than those formed on silicone. This is likely due the fact that the polymer chains grow over time as polyacrylamide polymerizes, so shorter polymerization times means shorter chains and a less rigid gel [43].

The reason that polyacrylamide is slower to polymerize on silicone is likely due to the permeability of silicone. Oxygen inhibits the polymerization of polyacrylamide [43]. When the gel is formed on glass, there is little surface area exposed to the air, so the polymerization occurs quickly. For the silicone plate, a nitrogen atmosphere is required and the polymerization is still slower, possibly to due oxygen retained in the silicone (PDMS is similar to this silicone, and PDMS is very gas permeable [48]).

The variation in the storage moduli between different gels is significant. It is possible that this is the result of different degrees of mixing between the different batches. It is also possible

that different gels are exposed to different amounts of oxygen during the polymerization process, which could alter the polymerization [43].

The gels formed on the silicone plate were found to be smooth enough for our experiments. They are still rougher than those formed on glass, possibly due being formed on a material that is not as smooth to begin with. More sticking to the coverslip that gets removed could also be a factor. In the future, length scales longer than 25 μm may be considered in order to account for the potential effect of roughness across a whole aggregate instead of individual cells. Much work has been done studying the effects of nanoscale topography on cell behavior [49]. On less "rough" substrates, meaning substrates with smaller nanoscale topography, cell behavior has been shown to approach that of cells on smooth substrates [50]. However, this dependent on the particular topography, there does not appear to be a universal cutoff roughness below which substrates can be considered completely smooth [50]. Comparing cell behaviors known to be affected by roughness (such as shape and proliferation [47, 49]) between cells on gels formed on the silicone plate to cells on gels formed on glass could be an additional way to further validate the smoothness of these gels.

In summary, a procedure for attaching polyacrylamide gels to CellScale silicone plates is demonstrated. The gels produced from this method are characterized to determine their storage moduli and determine if their surface features were acceptable for experiments, which they were.

4. Future Work

4.1. Effect of Stretch on Apoptosis and Osteogenic Differentiation

Stretched aggregates and control aggregates cultured for 5 days will be stained with caspase will be analyzed. The area positive for caspase will be compared. It is expected that the cyclic stretch will elevate the stress state in the center of the aggregates and thereby reduce apoptosis. Markers for calcification and osteogenic differentiation will be similarly analyzed.

4.2. Traction Force Microscopy

Traction force microcopy will be used to estimate the stresses within the aggregate. The magnitude of the stress and its distribution will be compared for control and stretched aggregates. This will enable comparison of directly measured traction force data regarding cyclically stretched aggregates to previous work which modeled the traction stresses for cyclically stretched aggregates but measured the traction forces only for static aggregates [6].

4.3. Rheometry on Gels on PDMS Wells

Polymerizing polyacrylamide gel under different conditions can influence its stiffness [43]. Measurements of the storage modulus of the gels polymerized on the CellScale silicone plates were made with a rheometer (see Section 3.3.2). Gels polymerized on the larger PDMS wells will be similarly measured. This will require cutting 5 mm sections of the gels out.

4.4. Micropatterning with CellScale

Being able to create aggregates on the CellScale silicone plate will enable much higher throughput experiments. To create these aggregates, several 5 mm circular coverslips will be stamped with the micropatterned protein islands instead of one 18 mm square coverslip. The circular coverslips will be used on top of the gel when it is polymerizing.

Conclusion

A procedure which can micropattern collagen onto polyacrylamide and simultaneously bind the polyacrylamide to PDMS is optimized and implemented here. The procedure successfully produces aggregates approximately 25% of the time, produced approximately 10 aggregates per well when successful. It is shown the aggregates can be stretched using this system and that apoptosis in the aggregates can be measured. It was found that culturing aggregates for 5 days was required to generate useful levels of apoptosis in the aggregates. A procedure to bind polyacrylamide gels to a commercially available multi-well stretchable silicone plate is optimized. The storage modulus of the gels is measured with a rheometer, and it is found that the storage modulus of the gels formed on the silicone plate is higher than gels polymerized in the rheometer. This indicates that polymerization conditions must be accounted for when characterizing the mechanical properties of the gels. Finally, the surfaces of gels formed on the silicone plate are scanned and it is found that cells or aggregates on the center of the gels

References

1. Willis, M.H., Jonathon W.; Stone, James R.; , *Cellular and Molecular Pathobiology of Cardiovascular Disease* 2014: Academic Press.

2. Fisher, C.I., J. Chen, and W.D. Merryman, Calcific nodule morphogenesis by heart valve interstitial cells is strain dependent, *Biomech Model Mechanobiol*. 12(1): 5-17, 2013.

3. Balachandran, K., et al., Elevated cyclic stretch induces aortic valve calcification in a bone morphogenic protein-dependent manner, *Am J Pathol*. 177(1): 49-57, 2010.

4. Chen, J.H., C.A. Simmons, and D.A. Towler, Cell-matrix interactions in the pathobiology of calcific aortic valve disease: critical roles for matricellular, matricrine, and matrix mechanics cues, *Circ Res*. 108(12): 1510-24, 2011.

5. Cirka, H.A., et al., Reproducible in vitro model for dystrophic calcification of cardiac valvular interstitial cells: insights into the mechanisms of calcific aortic valvular disease, *Lab Chip*. 17(5): 814-829, 2017.

6. Li, B., et al., Spatial patterning of cell proliferation and differentiation depends on mechanical stress magnitude, *J Biomech*. 42(11): 1622-7, 2009.

7. Krishnan, R., et al., Reinforcement versus fluidization in cytoskeletal mechanoresponsiveness, *PLoS One*. 4(5): e5486, 2009.

8. Sears, C. and R. Kaunas, The many ways adherent cells respond to applied stretch, *J Biomech*. 49(8): 1347-1354, 2016.

9. Wang, J.H. and B.P. Thampatty, An introductory review of cell mechanobiology, *Biomech Model Mechanobiol*. 5(1): 1-16, 2006.

10. Ghazanfari, S., M. Tafazzoli-Shadpour, and M.A. Shokrgozar, Effects of cyclic stretch on proliferation of mesenchymal stem cells and their differentiation to smooth muscle cells, *Biochem Biophys Res Commun*. 388(3): 601-5, 2009.

11. Chen, K., et al., Role of boundary conditions in determining cell alignment in response to stretch, *Proc Natl Acad Sci U S A*. 115(5): 986-991, 2018.

12. Wen, J.H., et al., Interplay of matrix stiffness and protein tethering in stem cell differentiation, *Nat Mater*. 13(10): 979-87, 2014.

13. Bhadriraju, K. and L.K. Hansen, Extracellular matrix- and cytoskeleton-dependent changes in cell shape and stiffness, *Exp Cell Res*. 278(1): 92-100, 2002.

14. Simmons, C.S., A.J. Ribeiro, and B.L. Pruitt, Formation of composite polyacrylamide and silicone substrates for independent control of stiffness and strain, *Lab Chip*. 13(4): 646-9, 2013.

15. Casares, L., et al., Hydraulic fracture during epithelial stretching, *Nat Mater*. 14(3): 343-51, 2015.

16. Steucke, K.E., et al., Empirically Determined Vascular Smooth Muscle Cell Mechano-Adaptation Law, *J Biomech Eng*. 139(7), 2017.

17. *MCFX High throughput uniaxial stimulation of cell cultures with real-time imaging.* [cited 2020 3/20/2020]; Available from: https://cellscale.com/products/mcfx/.

18. Alom Ruiz, S. and C.S. Chen, Microcontact printing: A tool to pattern, *Soft Matter*. 3(2): 168-177, 2007.

19. Goldblatt, Z.E., et al., Heterogeneity Profoundly Alters Emergent Stress Fields in Constrained Multicellular Systems, *Biophysical Journal*. 118(1): 15-25, 2020.

20. Style, R.W., et al., Traction force microscopy in physics and biology, *Soft Matter*. 10(23): 4047-55, 2014.

21. Kenry, et al., Viscoelastic Effects of Silicone Gels at the Micro- and Nanoscale, *Procedia IUTAM*. 12: 20-30, 2015.

22. S. Karpitschka, J.E., A. Pandey, and J. H. Snoeijer, Cusp-Shaped Elastic Creases and Furrows, *Phys. Rev. Lett.* . 119, 2017.

23. Hutcheson, J.D., et al., Intracellular Ca(2+) accumulation is strain-dependent and correlates with apoptosis in aortic valve fibroblasts, *J Biomech*. 45(5): 888-94, 2012.

24. Wipff, P.J., et al., The covalent attachment of adhesion molecules to silicone membranes for cell stretching applications, *Biomaterials*. 30(9): 1781-9, 2009.

25. Mertz, A.F., et al., Scaling of traction forces with the size of cohesive cell colonies, *Phys Rev Lett*. 108(19): 198101, 2012.

26. Damljanovic, V., B.C. Lagerholm, and K. Jacobson, Bulk and micropatterned conjugation of extracellular matrix proteins to characterized polyacrylamide substrates for cell mechanotransduction assays, *Biotechniques*. 39(6): 847-51, 2005.

27. Hynd, M.R., et al., Directed cell growth on protein-functionalized hydrogel surfaces, *J Neurosci Methods*. 162(1-2): 255-63, 2007.

28. Sarker, B., C. Walter, and A. Pathak, Direct Micropatterning of Extracellular Matrix Proteins on Functionalized Polyacrylamide Hydrogels Shows Geometric Regulation of Cell–Cell Junctions, *ACS Biomaterials Science & Engineering*. 4(7): 2340-2349, 2018.

29. Rape, A.D., W.H. Guo, and Y.L. Wang, The regulation of traction force in relation to cell shape and focal adhesions, *Biomaterials*. 32(8): 2043-51, 2011.

30. Polio, S.R., et al., A micropatterning and image processing approach to simplify measurement of cellular traction forces, *Acta Biomater*. 8(1): 82-8, 2012.

31. Tang, X., M.Y. Ali, and M.T. Saif, A Novel Technique for Micro-patterning Proteins and Cells on Polyacrylamide Gels, *Soft Matter*. 8(27): 7197-7206, 2012.

32. Krishnan, R., et al., Substrate stiffening promotes endothelial monolayer disruption through enhanced physical forces, *Am J Physiol Cell Physiol*. 300(1): C146-54, 2011.

33. Wang, N., et al., Micropatterning tractional forces in living cells, *Cell Motil Cytoskeleton*. 52(2): 97-106, 2002.

34. Moussus, M., et al., Intracellular stresses in patterned cell assemblies, *Soft Matter*. 10(14): 2414-23, 2014.

35. Bernard, A., et al., Microcontact Printing of Proteins, *Advanced Materials*. 12(14): 1067-1070, 2000.

36. Yip, C.Y., et al., Calcification by valve interstitial cells is regulated by the stiffness of the extracellular matrix, *Arterioscler Thromb Vasc Biol*. 29(6): 936-42, 2009.

37. He, S., et al., Dissecting Collective Cell Behavior in Polarization and Alignment on Micropatterned Substrates, *Biophys J*. 109(3): 489-500, 2015.

38. Liu, C., et al., Mechanics of Cell Mechanosensing on Patterned Substrate, *Journal of Applied Mechanics*. 83(5), 2016.

39. Bashirzadeh, Y., et al., Mechanical response of an epithelial island subject to uniaxial stretch on a hybrid silicone substrate, *Cell Mol Bioeng*. 12(1): 33-40, 2019.

40. Coburn, L., et al., Contact inhibition of locomotion and mechanical cross-talk between cell-cell and cell-substrate adhesion determine the pattern of junctional tension in epithelial cell aggregates, *Mol Biol Cell*. 27(22): 3436-3448, 2016.

41. Tambe, D.T., et al., Collective cell guidance by cooperative intercellular forces, *Nat Mater*. 10(6): 469-75, 2011.

42. Ribeiro, A.J., et al., For whom the cells pull: Hydrogel and micropost devices for measuring traction forces, *Methods*. 94: 51-64, 2016.

43. Menter, P., Acrylamide Polymerization — A Practical Approach, *Bio-Rad Tech Note*, 2000.

44. Denisin, A.K. and B.L. Pruitt, Tuning the Range of Polyacrylamide Gel Stiffness for Mechanobiology Applications, *ACS Appl Mater Interfaces*. 8(34): 21893-902, 2016.

45. Wang, Y.L. and R.J. Pelham Jr, Preparation of a flexible, porous polyacrylamide substrate for mechanical studies of cultured cells, *Methods in Enzymology*. 298: 489-496, 1998.

46. Yeung, T., et al., Effects of substrate stiffness on cell morphology, cytoskeletal structure, and adhesion, *Cell Motil Cytoskeleton*. 60(1): 24-34, 2005.

47. Bacakova, L., et al., Modulation of cell adhesion, proliferation and differentiation on materials designed for body implants, *Biotechnol Adv*. 29(6): 739-67, 2011.

48. Xu, L., et al., Vacuum-driven power-free microfluidics utilizing the gas solubility or permeability of polydimethylsiloxane (PDMS), *Lab Chip*. 15(20): 3962-79, 2015.

49. Kim, D.-H., et al., Matrix nanotopography as a regulator of cell function, *The Journal of Cell Biology*. 197(3): 351-360, 2012.

50. Loesberg, W.A., et al., The threshold at which substrate nanogroove dimensions may influence fibroblast alignment and adhesion, *Biomaterials*. 28(27): 3944-51, 2007.

Appendix 1: Initial Protocol for Binding Polyacrylamide Gel to CellScale Silicone Plate

Materials:

40% Acrylamide

2% Bisacrylamide

HEPES Buffer

TEMED

1% Ammonium Persulfate (APS)

1% APTMS ((3-aminopropyl) trimethoxysilane)

0.5% Glutaraldehyde

CellScale Silicone Plate

DI Water

Ethanol

Procedure:

- Mix gel precursor solution. For stiff gels: 100 µL Acrylamide, 19.6 µL Bisacrylamide, 180 µL HEPES Buffer, 1 µL TEMED. For soft gels: 25 µL Acrylamide, 17.9 µL Bisacrylamide, 257 µL HEPES Buffer, 1 µL TEMED.
- Clean silicone plate by sonicating in ethanol for approximately 5 minutes
- Dry in 60 ^{o}C oven
- Plasma treat silicone for 2 minutes at 100 W
- Pipette 100 µL APTMS into wells, leave for 5 minutes, remove APTMS
- Pipette 100 µL Glutaraldehyde into wells, leave for 5 minutes, remove Glutaraldehyde
- Dry with nitrogen gun

- Add 33 µL APS to precursor solution to initiate polymerization
- Pipette a 2.5 µL droplet of polymerizing gel solution into each well being used
- Place 5 mm coverslips on each droplet
- Place silicone plate in vacuum chamber, apply vacuum for 30-45 seconds
- Using nitrogen gun, refill vacuum chamber with nitrogen
- Wait 45 minutes for stiff gels, 1.5 hours for soft gels
- Remove gels from vacuum chamber, soak in DI water for a few minutes
- Remove coverslips

Appendix 2: Final Protocol for Binding Polyacrylamide Gel to CellScale Silicone Plate

Materials:

40% Acrylamide

2% Bisacrylamide

HEPES Buffer

TEMED

1% Ammonium Persulfate (APS)

1% APTMS ((3-aminopropyl) trimethoxysilane)

0.5% Glutaraldehyde

CellScale Silicone Plate

DI Water

Ethanol

Procedure:

- Mix gel precursor solution. For stiff gels: 100 µL Acrylamide, 19.6 µL Bisacrylamide, 180 µL HEPES Buffer, 1 µL TEMED. For soft gels: 25 µL Acrylamide, 17.9 µL Bisacrylamide, 257 µL HEPES Buffer, 1 µL TEMED.
- Clean silicone plate by sonicating in ethanol for approximately 5 minutes
- Dry in 60 ^{o}C oven
- Plasma treat silicone for 2 minutes at 100 W
- Pipette 100 µL APTMS into wells, leave for 5 minutes, remove APTMS
- Pipette 100 µL Glutaraldehyde into wells, leave for 5 minutes, remove Glutaraldehyde
- Dry with nitrogen gun
- Add 33 µL APS to precursor solution to initiate polymerization
- Pipette a 4 µL droplet of polymerizing gel solution into each well being used
- Place 5 mm coverslips on each droplet
- Place silicone plate in vacuum chamber
- Flow nitrogen through the chamber using nitrogen gun for 60 seconds, then close valve
- Wait 45 minutes for stiff gels, 1.5 hours for soft gels
- Remove gels from vacuum chamber, soak in DI water for 30 minutes for stiff gels, 1 hour for soft gels
- Remove coverslips.

Appendix 3: Storage and Loss Modulus Rheometry Measurements

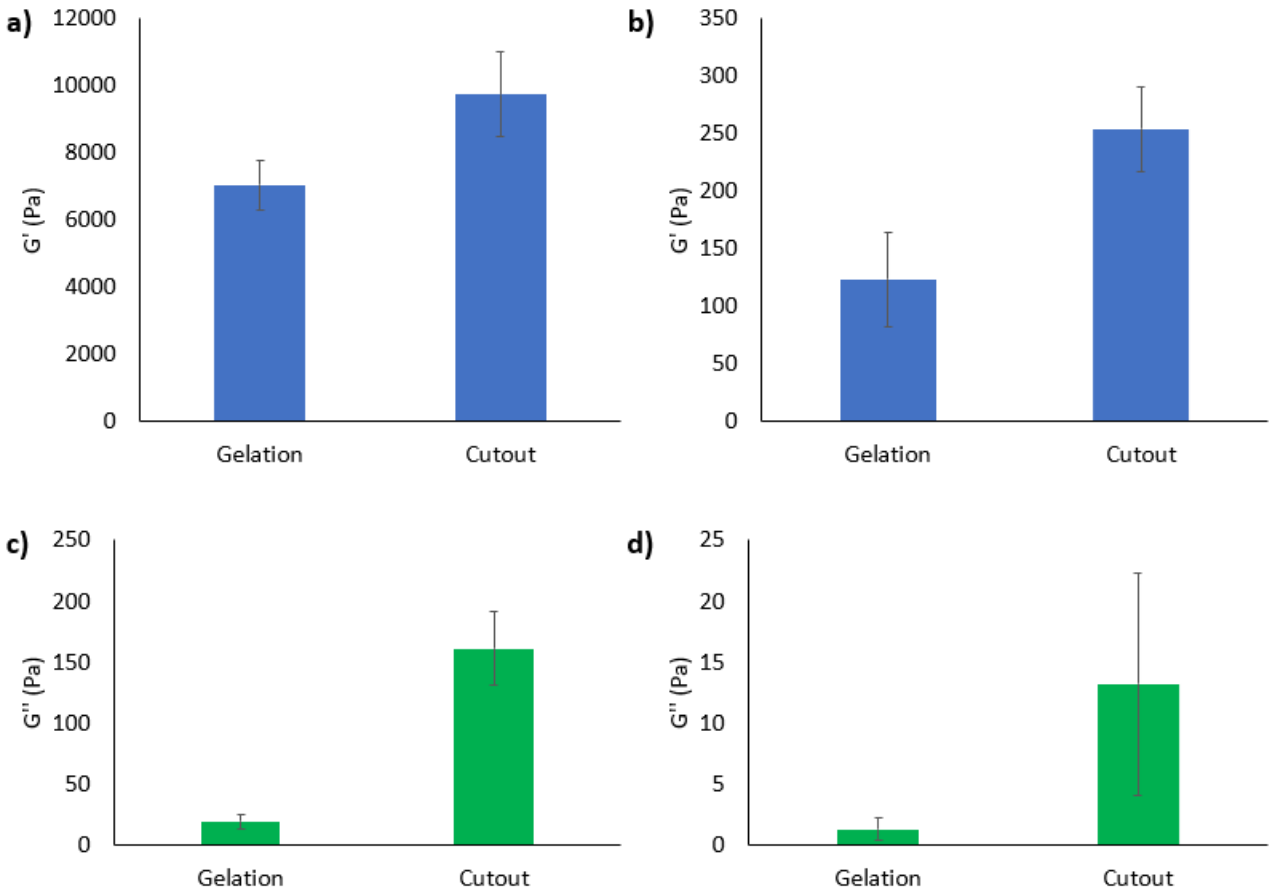

Figure 15: The storage modulus (a, b) and loss modulus (c, d) of different gel formulations, with higher modulus gels (a,c) on the left and lower modulus gels (b, d) on the right (referred to elsewhere as stiff gels and soft gels), polymerized under different conditions - either on the glass base of the rheometer (gelation) or on the CellScale silicone plate (cutout, because the base of the wells with the attached gel were cut out from the plate). Error bars indicate standard deviation. The loss moduli are much lower than the storage moduli, indicating that the gels behave mainly elastically.